Supporting Information

An Experimental and Theoretical Study on Isotopic Surface-Enhanced Raman Spectroscopy for Surface Catalytic Coupling Reaction on Silver Electrodes

Meng Zhang, Liu-Bin Zhao, Wen-Li Luo, Ran Pang, Cheng Zong, Jian-Zhang Zhou, Bin Ren, Zhong-Qun Tian,* and De-Yin Wu*

S1. High pressure liquid chromatography and mass spectrometry of synthesis products.

In order to further purify the as-prepared product, high performance liquid chromatography combined with mass spectroscopy (HPLC-MS) (Thermo Finnigan LCQ Mass) was used to detect and separate the main and possible minor products effectively. Chromatographic separation of PATP-d4 and by-products was performed on a C-18 column with a mobile phase consisting of 70% methyl alcohol and 30% water containing 0.1% formic acid, pumped at a flow rate of 1 mL min-1. Two distinct broad peaks are shown during the total run time of 14.78 min in the mass spectrum. One is from 7.31 to 8.06 min and the other is from 11.17 to 12.33 min. On the basis of the corresponding realtime mass spectra, the peak at ca. 159.8 can be easily ascribed to PCNB-d4, and the other strong peak at 257.4 is due to the formation of APDS-d8, $(APDS\text{-}d8)^{+}$ and $(APDS\text{-}d8)^{2+}(CH_3OH)_2$. This is a proof that PATP-d0 or PATP-d4 molecules which include thiol group easily couple to generate the dimer compound bis(p-aminophenyl) disulfide (APDS) or bis(p-aminophenyl-d8) disulfide (APDS-d8). The extracted product during the retention time of 11.17 ~ 12.33 min was collected as the purified product.

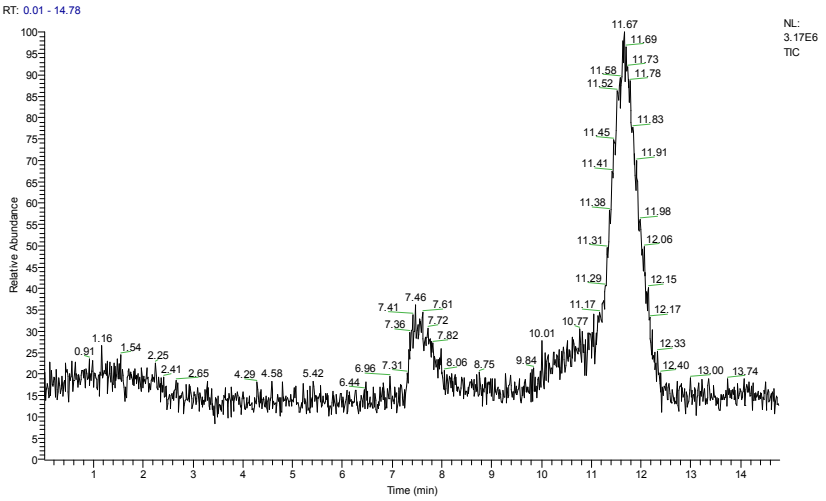

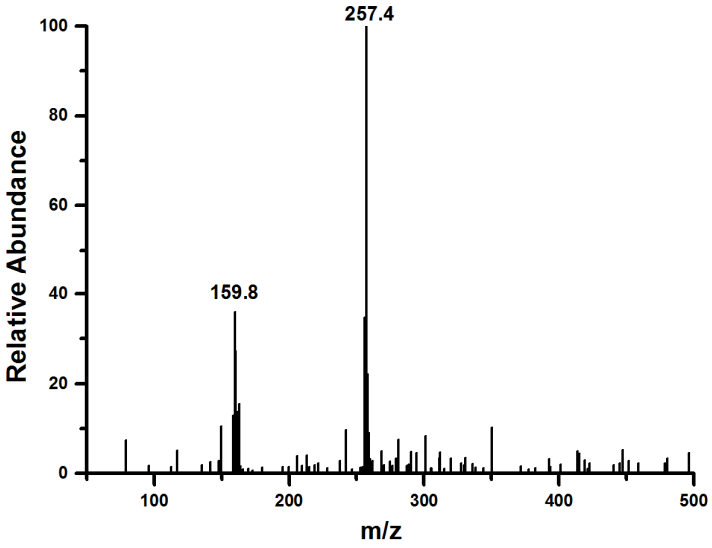

Figure S1. HPLC and MS spectra of the as-prepared product.

S2. Characterization of synthesized Ag NPs.

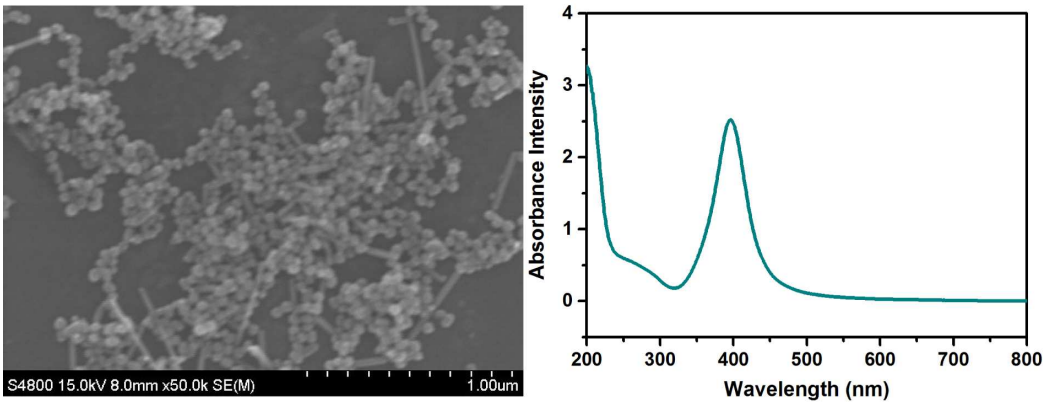

Figure S2. (a) SEM image and (b) UV-visible extinction spectra of synthesized Ag NPs. The particle size is about 2 ~ 10 nm, and the absorption peak locates at 396 nm.

S3. Table S1. Comparison of Theoretical and Experimental Frequencies of Selected Fundamental Vibrational Bands of PATP-d0, PATP-^{15}N, and PATP-d4 within the Frequency Range of 800 ~ 1700 cm^{-1}.

PATP		PATP-^{15}N		PATP-d4	
Theory /cm^{-1}	Assignment (PED %)	Theory /cm^{-1}	Assignment (PED %)	Theory /cm^{-1}	Assignment (PED %)
824	$\nu_{CC}(34)+\nu_{CN}(18)+\alpha_{CCC}(13)$	820	$\nu_{CC}(31)+\nu_{CN}(16)+\alpha_{CCC}(13)$	770	$\nu_{CC}(33)+\nu_{CN}(12)+\alpha_{CCC}(10)+\beta_{CD}(27)$
				872	$\nu_{CC}(22)+\alpha_{CCC}(12)+\beta_{CD}(47)$
904	$\beta_{SH}(70)$	904	$\beta_{SH}(70)$	910	$\beta_{SD}(90)$
				1026	$\nu_{CS}(19)+\alpha_{CCC}(44)$
1088	$\nu_{CC}(45)+\nu_{CS}(19)$	1088	$\nu_{CC}(45)+\nu_{CS}(19)$		

1279	$\nu_{CN}(53)$	1273	$\nu_{CN}(52)$	1215	$\nu_{CN}(39)+\nu_{CC}(34)$
1492	$\nu_{CC}(20)+\beta_{CH}(56)$	1491	$\nu_{CC}(20)+\beta_{CH}(56)$		
				1404	$\nu_{CC}(47)+\nu_{CN}(23)$
1607	$\nu_{CC}(37)+\delta_{NH2}(13)$	1606	$\nu_{CC}(37)+\delta_{NH2}(16)$	1581	$\nu_{CC}(46)$
1633	$\delta_{NH2}(86)$	1627	$\delta_{NH2}(83)$	1631	$\nu_{CC}(95)$

S4. Comparison of simulated Raman spectra of APDS using different basis sets.

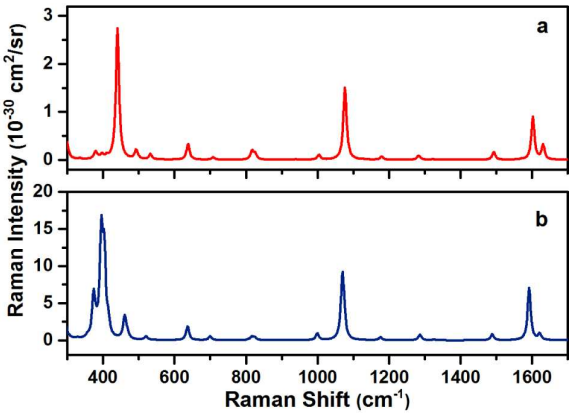

Figure S3. Simulated Raman spectra of APDS by using (a) the 6-311+G(3df, 3p) level, and (b) the 6-311+G(d, p) level. An excitation wavelength of 532 nm and a line width of 10 cm^{-1} were used.

S5. Structure and Raman spectra of TAB and its isotopologues.

Before investigating isotopic effects on the SERS of DMAB, we first studied its parent molecule, trans-azobenzene (TAB), to check the reliability of theoretical methods in predicting the isotopic effects on vibrational spectroscopy. The 66 fundamentals of TAB span the representation Γ = 23Ag + 10Bg + 11Au + 22Bu vibrations. Due to the presence of the inversion center in TAB, 33 centrosymmetric modes are Raman active whereas 33 non-centrosymmetric modes are IR active. The 33 Raman active modes of TAB consist of 23 in-plane (Ag) and 10 out-of-plane (Bg) vibrations. The 33 IR active modes include 22 in-plane (Bu) and 11 out-of-plane (Au) vibrations. Raman spectrum of TAB within wavenumber range of 1000 to 1600 cm^{-1} gives intense characteristic signals arising from C-N, N-N, C-C stretching modes and C-H in-plane bending modes. Figure S4 shows the simulated Raman spectra of TAB and its isotopologues by using PW91PW91/6-311+G(d,p). Previous studies indicate that the generalized gradient approximation functional PW91PW91 is good at predicting the geometry structure and vibrational spectrum of TAB. However, the widely used hybrid exchange-correlation functional B3LYP overestimates the N=N bond strength. This overestimation leads to a blue shift of the vibrational frequencies involved in the N=N stretching.

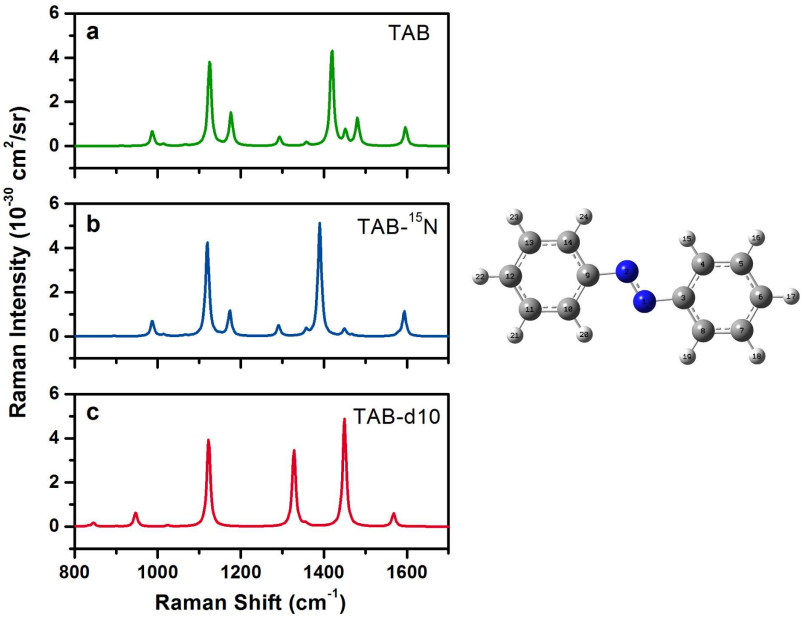

Figure S4. Simulated Raman spectra of (a) TAB, the isotopologues (b) TAB-^{15}N and (c) TAB-d10 by using PW91PW91/6-311+G(d, p). An excitation wavelength of 632.8 nm and a line width of 10 cm^{-1} were used.

As seen in Figure S4, the 1419 cm^{-1} peak of TAB corresponds to the main azo N=N stretching. The calculated frequency red-shifts by 29 cm^{-1} (1419 to 1390 cm^{-1}) when both the N atoms of the azo group are substituted by ^{15}N. Interestingly, the ν_{NN} mode is also influenced by complete deuteration as evidenced by the shift of 31 cm^{-1} (1419 to 1450 cm^{-1}). These results are consistent with the experimental data where the shift is 27 cm^{-1}, which is observed for TAB-^{15}N and TAB-d10, respectively.[1] This is also in accordance to the theoretical prediction by Biswas and Umapathy by using BP86 and Armstrong et al. and Fliegl et al. by using MP2 method.[2-4] A detailed PED analysis for TAB, TAB-^{15}N, and TAB-d10 is presented in Table S2. As observed in the Figure S4b, the decrease in frequency upon ^{15}N substitution of the main azo ν_{NN} stretching mode at 1419 cm^{-1} is due to the effective increase in reduced mass. It is also noticed that the vibrational coupling between the ν_{NN} and β_{CH} significantly weakens in TAB-^{15}N. The increase in frequency upon deuteration can be explained as the reduced contribution from the β_{CH}.[2-3] However, such interpretation is in contrast to Uno et al. who investigate the isotopic effects on some azobenzene derivatives such as DMAB, p-dimethylaminoazobenzene, and p-hydroxyazobenzene.[5-6] The authors considered the blue shift of azo ν_{NN} stretching mode is due to the stronger coupling between ν_{NN} and deuterated ring.

The main Raman active modes for the symmetric C-N stretching of TAB calculated to be at 1125 and 1176 cm^{-1} are quite close to experimental observation at 1146 and 1184 cm^{-1}, respectively.[7] According to the calculation, it is observed that the 1125 cm^{-1} peak undergoes a downward shift of 6 cm^{-1} upon ^{15}N substitution, whereas the experimentally observed shift is 5 cm^{-1}, while the 1176 cm^{-1} peak disappears due to deuteration (TAB-d10). Furthermore, it is found that a new peak appears at 1328 cm^{-1} which is a complex normal mode mixed with ν_{CC}, ν_{CN}, and ν_{NN} stretching in TAB-d10, and this mode is also experimentally observed.[1, 7]

Finally, we notice that the ν_{CC} mode at 1596 cm^{-1} is also influenced by isotopic effects which does

not attract much attention by previous studies.[2-3] It is observed that this mode just shows a slight frequency shift ($\Delta \sim 2$ cm^{-1}) by ^{15}N substitution, however, a significant shift to lower wavenumber by 28 cm^{-1} upon deuteration (TAB-d10). Experimentally, the frequency shift is about 32 cm^{-1}. The red shift of the ν_{CC} mode can be understood from PED analysis, that is, a decrease contribution from β_{CD} in TAB-d10.

Table S2. Harmonic Frequencies and PED Analysis for Selected Fundamental Vibrational Modes of TAB and Its Isotopic Derivatives within the Frequency Range of 1000 ~ 1700 cm^{-1}.

TAB			TAB-^{15}N			TAB-d10		
Theory /cm^{-1}	Exp. /cm^{-1}	Assignment (PED %)	Theory /cm^{-1}	Exp. /cm^{-1}	Assignment (PED %)	Theory /cm^{-1}	Exp. /cm^{-1}	Assignment (PED %)
1125	1146	$\nu_{CN}(25)+\beta_{CH}(32)$	1119	1141	$\nu_{CN}(28)+\beta_{CH}(30)$	1122	1139	$\nu_{CN}(43)+\beta_{CD}(13)$
1176	1184	$\nu_{CN}(22)+\beta_{CH}(43)$	1173	1181	$\nu_{CN}(18)+\beta_{CH}(48)$			
						1328	1351	$\nu_{CC}(47)+\nu_{CN}(11)+\nu_{NN}(8)$
1419	1439	$\nu_{NN}(44)+\beta_{CH}(33)$	1390	1412	$\nu_{NN}(69)+\beta_{CH}(18)$	1450	1466	$\nu_{NN}(72)+\beta_{CD}(4)$
1452	1471	$\beta_{CH}(53)$	1449	1464	$\beta_{CH}(23)$			
1596	1590	$\nu_{CC}(43)+\beta_{CH}(16)$	1594	1591	$\nu_{CC}(43)+\beta_{CH}(17)$	1568	1558	$\nu_{CC}(57)+\beta_{CD}(7)$

The above discussions show that the present calculation method can well predict isotopic effects on the vibrational frequency shift and Raman intensity of TAB. Herein, we can make proper theoretical predictions on the isotopic effects on Raman spectra of other modeling molecules.

S6. Comparison of simulated Raman spectra of PATP isotopologues interacting with different sizes of silver clusters.

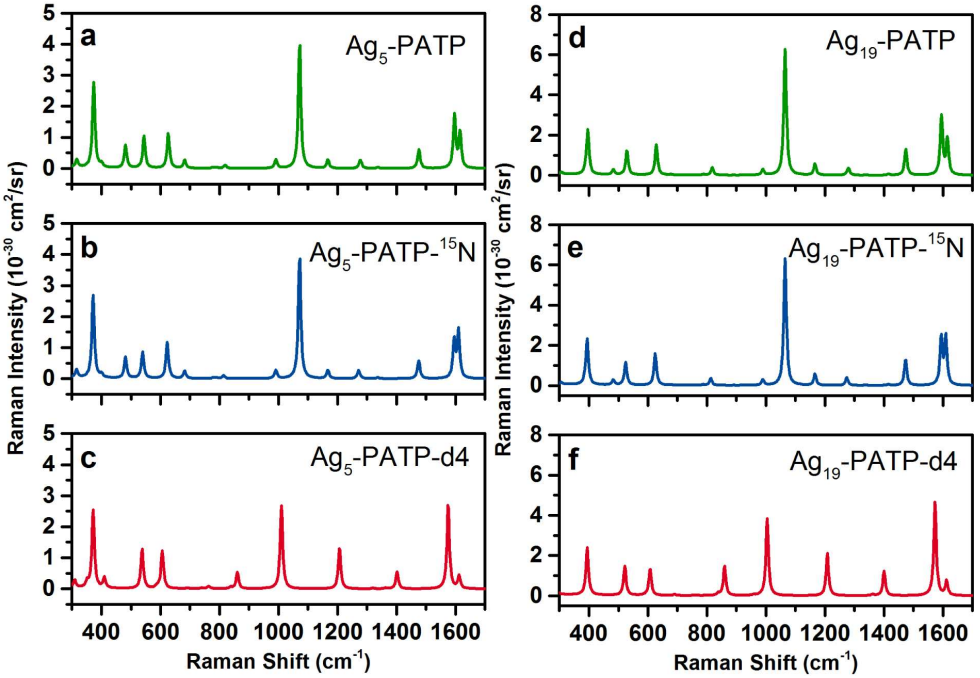

Figure S5. Calculated Raman spectra of (a) Ag_5-PATP, (b) Ag_5-PATP-^{15}N, (c) Ag_5-PATP-d4, (d)

Ag_{19}-PATP, (e) Ag_{19}-PATP-^{15}N, and (f) Ag_{19}-PATP-d4 by using B3LYP/6-311+G(d,p). The excitation wavelength used is 532 nm with a Lorentzian line width of 10 cm^{-1}.

S7. Vibrational coupling of N=N stretching and C-H in-plane bending modes in DMAB and its isotopologues.

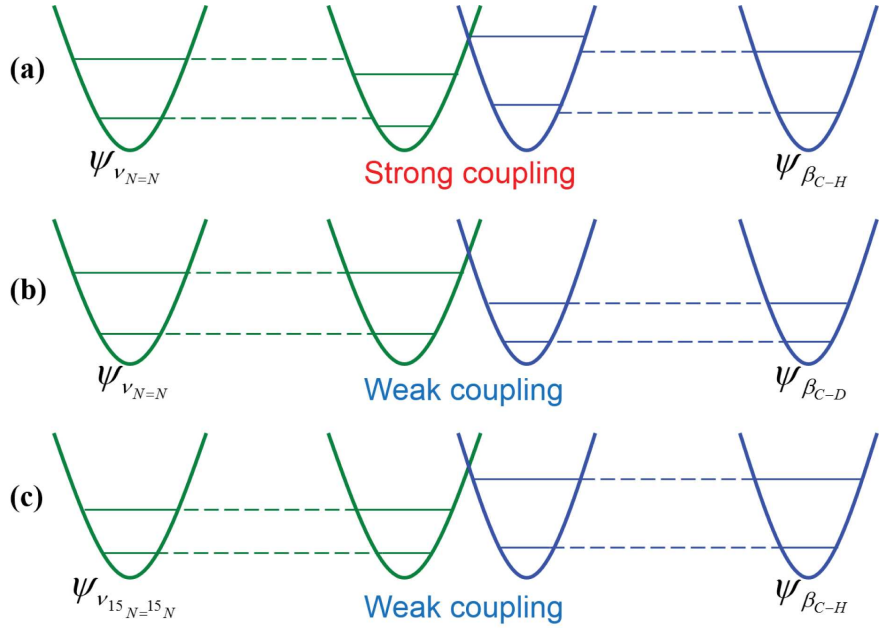

Scheme S1. Vibrational coupling of N=N stretching and C-H in-plane bending modes in DMAB and its isotopologues: (a) strong coupling of the ν_{NN} and the β_{CH} modes, (b) weak coupling of the ν_{NN} and the β_{CD} modes, and (c) weak coupling of the $\nu(^{15}N=^{15}N)$ and the β_{CH} modes.

The vibrational coupling of the two modes distinctly influences the relative intensities and vibrational frequency shifts of Raman peaks. Taking the coupling interaction of ν_{NN} and β_{CH} or β_{CD} into consideration, the isotopic substitution of N or H atoms can easily change the vibrational levels of N=N or C-H/C-D bonds through tuning the reduced masses. Without the isotope substitution, the vibrational levels of the N=N stretching and the C-H bending are close, thus the vibrational coupling strength of ν_{NN} and β_{CH} modes becomes significant, leading to changes of the Raman bands (see Scheme 2a). For non-isotopically substituted DMAB, the ν_{NN} stretching and the β_{CH} bending are strongly coupled so that the ν_{NN} stretching contributes to two intense Raman bands at 1392 and 1428 cm^{-1}. After deuteration of four hydrogen atoms in the benzene ring, the vibrational level of the C-D bending becomes far from the N=N stretching. The case was showed in Scheme S1(b), where the coupling strength with the ν_{NN} stretching also becomes weak because the vibrational frequency of the β_{CD} bending in DMAB-d8 shifts to a lower wavenumber, resulting in only one strong Raman peak of the N=N stretching left at 1426 cm^{-1}. As shown in Scheme S2c, by the ^{15}N substitution, the vibrational level of the $^{15}N=^{15}N$ stretching becomes lower than the phenyl C-H in-plane bending vibration, so that the two vibrational levels no longer match well. It leads to the weaker vibrational coupling between the ν_{NN} stretching and the β_{CH} bending and thus the ν_{NN} stretching frequency shifts to 1367 cm^{-1} compared than that in DMAB. Thus one can see only one intense Raman peak at 1367 cm^{-1} which mainly comes from the ν_{NN} stretching.

REFERENCES

1. Meic, Z.; Baranovic, G.; Smrecki, V.; Novak, P.; Keresztury, G.; Holly, S., Vibrational Coupling in Trans-Azobenzene and Its Isotopomers. *J. Mol. Struct.* **1997**, *408-409*, 399-403.
2. Biswas, N.; Umapathy, S., Density Functional Calculations of Structures, Vibrational Frequencies, and Normal Modes of Trans- and Cis-Azobenzene. *J. Phys. Chem. A* **1997**, *101*, 5555-5566.
3. Armstrong, D. R.; Clarkson, J.; Smith, W. E., Vibrational Analysis of Trans-Azobenzene. *J. Phys. Chem.* **1995**, *99*, 17825-17831.
4. Fliegl, H.; Köhn, A.; Hättig, C.; Ahlrichs, R., Ab Initio Calculation of the Vibrational and Electronic Spectra of Trans- and Cis-Azobenzene. *J. Am. Chem. Soc.* **2003**, *125*, 9821-9827.
5. Uno, T.; Lee, H.; Saito, Y.; Machida, K., Resonance Raman Spectra of P-Hydroxyazobenzene and Its Ring-Deuterated Derivatives. *Spectrochimica Acta, Part A: Molecular and Biomolecular Spectroscopy* **1976**, *32A*, 1319-1322.
6. Uno, T.; Kim, B.; Saito, Y.; Machida, K., Resonance Raman Spectra of Some Ring-Deuterated Derivatives of P-Aminoazobenzene and P-Dimethylaminoazobenzene. *Spectrochimica Acta, Part A: Molecular and Biomolecular Spectroscopy* **1976**, *32A*, 1179-1183.
7. Kellerer, B.; Hacker, H. H.; Brandmueller, J., Structure of Azobenzene and Tolane in Solution. Raman Spectra of Azobenzene, Azobenzene-D10, P,P'-Azobenzene-D2, Azobenzene-15N2, and Tolane. *Ind. J. Pure Appl. Phys.* **1971**, *9*, 903-909.